AJNR

Effect of Voxel Position on Single-Voxel MR Spectroscopy Findings

Peter E. Ricci, Alan Pitt, Paul J. Keller, Stephen W. Coons and Joseph E. Heiserman

AJNR Am J Neuroradiol 2000, 21 (2) 367-374
http://www.ajnr.org/content/21/2/367

AJNR Am J Neuroradiol 21:367–374, February 2000

Effect of Voxel Position on Single-Voxel MR Spectroscopy Findings

Peter E. Ricci, Alan Pitt, Paul J. Keller, Stephen W. Coons, and Joseph E. Heiserman

BACKGROUND AND PURPOSE: **Single-voxel MR spectroscopy is a widely used tool for evaluating brain tumors. Although extensive data are available on the MR spectral appearance of tumors, less is known about the effect of voxel position on the accuracy of single-voxel MR spectroscopy findings. The purpose of this study was to test the hypothesis that the accuracy of single-voxel MR spectroscopy in the categorization of lesions as either tumor or not tumor is dependent on voxel position.**

METHODS: **Fifty single-voxel MR spectra acquired with a fully automated stimulated-echo spectroscopy sequence were reviewed retrospectively in 43 patients with new or previously treated intra-axial brain tumors. Spectra were analyzed for the presence of choline, creatine, *N*-acetylaspartate (NAA), and lipid/lactate. Choline/creatine and NAA/creatine peak area ratios were assessed qualitatively. Lesions were grouped into one of three categories on the basis of spectral pattern: tumor, not tumor, or indeterminate. Results of MR spectroscopy were compared with the final histopathologic diagnosis.**

RESULTS: **Histologic confirmation was obtained in 19 patients; MR spectra were interpretable in 17 of those. MR spectra correctly categorized nine of 17 lesions (six tumor, three nontumor). All eight misdiagnosed lesions were tumors. When the MR spectroscopy voxel included the enhancing edge of the lesion, the spectra correctly categorized seven of eight lesions (four of five tumors and all three cases of radiation necrosis). When the MR spectroscopy voxel was positioned centrally within the lesion, the spectra correctly reflected histologic outcome in two of nine lesions (all tumors).**

CONCLUSION: **The reliability of single-voxel MR spectroscopy findings is dependent on voxel position. Spectra obtained from voxels at the enhancing edge of a tumor more accurately reflect lesion histopathology than do spectra obtained from the lesion center, even if the centrally placed voxels contain solidly enhancing tissue.**

Hydrogen proton MR spectroscopy is a powerful technique that has been used to noninvasively evaluate tissue metabolism in a wide variety of diffuse and focal CNS diseases. Brain tumors (1–15), abscesses (10, 16, 17), metabolic and neurodegenerative diseases (11, 18–20), focal lesions in AIDS patients (11, 21, 22), and more have been studied extensively. MR spectroscopy has also been used to evaluate the efficacy of brain tumor therapy and to evaluate radiotherapy-induced changes (11, 23–33).

Received June 18, 1999; accepted after revision August 23.

From the Departments of Neuroradiology (P.E.R., A.P., J.E.H.), MR Physics (P.J.K.), and Pathology (S.W.C.), Barrow Neurological Institute, Phoenix, AZ.

Presented at the annual meeting of the American Society of Neuroradiology, San Diego, May, 1999.

Address reprint requests to Joseph E. Heiserman, MD, PhD, Department of Neuroradiology, Barrow Neurological Institute, 350 W Thomas Rd, Phoenix, AZ 85013.

In general, proton spectroscopy has two forms: single-voxel MR spectroscopy and MR spectroscopic imaging. MR spectroscopic imaging, the more technically advanced technique, acquires spectra from numerous small voxels covering a large area of the brain. The small voxel size minimizes the effects of volume averaging, while the large volume of coverage ensures that heterogeneous lesions are adequately sampled. However, because of the complex shimming, long acquisition times, and complicated data processing, MR spectroscopic imaging has been largely confined to research centers with dedicated spectroscopists. In contrast, single-voxel MR spectroscopy acquisition and processing are typically fully automated; for that reason, it is simpler to implement and easier to use than MR spectroscopic imaging. These factors, and a substantially shorter scan time than that of MR spectroscopic imaging, have resulted in more widespread use of single-voxel MR spectroscopy at both research and clinical MR centers.

Unfortunately, the limited coverage of a lesion afforded by the use of one voxel and the volume averaging that results from the relatively large voxel size make single-voxel MR spectroscopy less desirable than MR spectroscopic imaging for the study of histologically heterogeneous lesions, as primary malignant gliomas typically are (34, 35). Placement of a voxel in a low grade or frankly malignant or necrotic region of the tumor may yield distinctly different MR spectroscopy results. Treated brain tumors are equally heterogeneous histologically and as such are prone to the same voxel position and volume averaging problems.

Despite the wealth of information available on the MR spectral appearance of tumors and radiotherapy-induced changes, little is known about the effect of voxel position on the accuracy of single-voxel MR spectroscopy results when evaluating such histologically heterogeneous lesions. The purpose of this study was to test the hypothesis that the accuracy of single-voxel MR spectroscopy in the categorization of lesions as either tumor or not tumor is dependent on voxel position.

Methods

We retrospectively reviewed 50 consecutive MR imaging and single-voxel proton MR spectroscopy studies in 43 patients with intra-axial brain tumors referred for imaging over an 8-month period by the neuro-oncology and neurosurgery services. From that population, 19 patients met the following inclusion criteria: presence of a new or previously treated intra-axial brain tumor, subsequent histologic confirmation of the MR spectroscopy findings by either open biopsy or surgical resection, and inclusion of the region studied by MR spectroscopy in the portion of the lesion that was resected or from which a biopsy sample was obtained.

All MR studies were performed on a commercially available 1.5-T unit. Conventional MR imaging performed before MR spectroscopy included sagittal T1-weighted (700/16 [TR/TE]), axial T1-weighted (800/18), and dual-echo T2-weighted (2500/30,90) spin-echo images, all with one excitation and a matrix size of 256 × 192. An axial fast fluid-attenuated inversion-recovery sequence (3300/110; inversion time, 1420) with two excitations and a matrix size of 256 × 192 was also performed. Sagittal and axial T1-weighted imaging was repeated after intravenous administration of 0.1 mmol/kg of gadodiamide (Omniscan, Nycomed, New York, NY).

MR spectroscopy studies were performed with the fully automated Proton Brain Exam-Single Voxel (PROBE-SV) software package (GE Medical Systems, Milwaukee, WI). No additional gradient shimming or water suppression was used other than that normally used during the automated prescan mode. To increase the probability of including the more histologically aggressive portions of the lesion and to minimize the volume of nontumor tissue in the voxel, all MR spectroscopy voxels were placed in an enhancing portion of the lesion, as identified on enhanced T1-weighted images. Spectra were acquired in the stimulated-echo acquisition mode (STEAM) with the following parameters: 1500/30; mixing time, 13.7 milliseconds; 192 signal averages. The short TE was selected to maximize detection of lipid breakdown products, which have short T1 and T2 relaxation times. Voxel volumes ranged from 4 to 8 cm^3. Total acquisition time was 5 minutes 40 seconds.

Two neuroradiologists evaluated each spectrum for the presence of choline (Cho)-containing compounds, total creatine (Cr), *N*-acetyl compounds (NAA), lipids, and lactate. Spectra obtained with an identical STEAM sequence from healthy volunteers and from the contralateral normal hemisphere in several patients were used for comparison. Using a qualitative pattern-recognition approach and the following guidelines, spectra were placed into one of three categories: tumor, not tumor, or indeterminate. Spectra characterized by elevation of Cho/Cr ratio above 2:1 and with reduction of NAA were considered consistent with tumor. Marked reduction (or complete absence) of Cho, Cr, and NAA levels in combination with a large lipid/lactate peak was considered compatible with tissue necrosis/no viable tumor. All other spectral patterns were considered indeterminate for the purposes of this study. Such qualitative evaluation of the spectra was based on results of previous studies that have applied a variety of pattern-recognition techniques to the analysis of tumor spectra (8, 13, 36–38). In several of those studies, investigators concluded that normal and abnormal spectra can be distinguished by means of pattern recognition alone (8, 13, 37).

TABLE 1: Summary of MR spectroscopy findings and histologic results

MR Spectroscopy Interpretation	Histologic Diagnosis		
	Tumor	Necrosis	Total
Tumor	6	0	6
No tumor	7	3	10
Indeterminate	1	0	1
Total	14	3	17

TABLE 2: Summary of MR spectroscopy and histologic results by voxel location

	No.	No. (%) of Correct MR Spectroscopy Findings	No. (%) of Incorrect MR Spectroscopy Findings
Voxel at edge (n = 8)		7 (88)	1 (12)
Tumor	5	4 (80)	1 (20)
Nontumor	3	3 (100)	0
Voxel in center/cavity (n = 9)		2 (22)	7 (78)
Tumor	9	2 (22)	7 (78)
Nontumor	0	0	0

Results

Nineteen patients met the inclusion criteria outlined above. In two patients with surgically proved radiation necrosis, the spectra were considered uninterpretable because of either failed water suppression or high background noise. Both were eliminated from the subsequent analysis. The study population therefore consisted of 17 patients (eight women, nine men) with new (n = 11) or previously treated (n = 6) brain tumors. Average age was 55 years (range, 42 to 70 years). Results are summarized in Tables 1 and 2.

Overall, nine (53%) of the 17 lesions were correctly diagnosed by means of MR spectroscopy, including six (43%) of 14 tumors and three (100%) of three cases of radiation necrosis (Table 1). Eight (47%) of the 17 lesions were incorrectly catego-

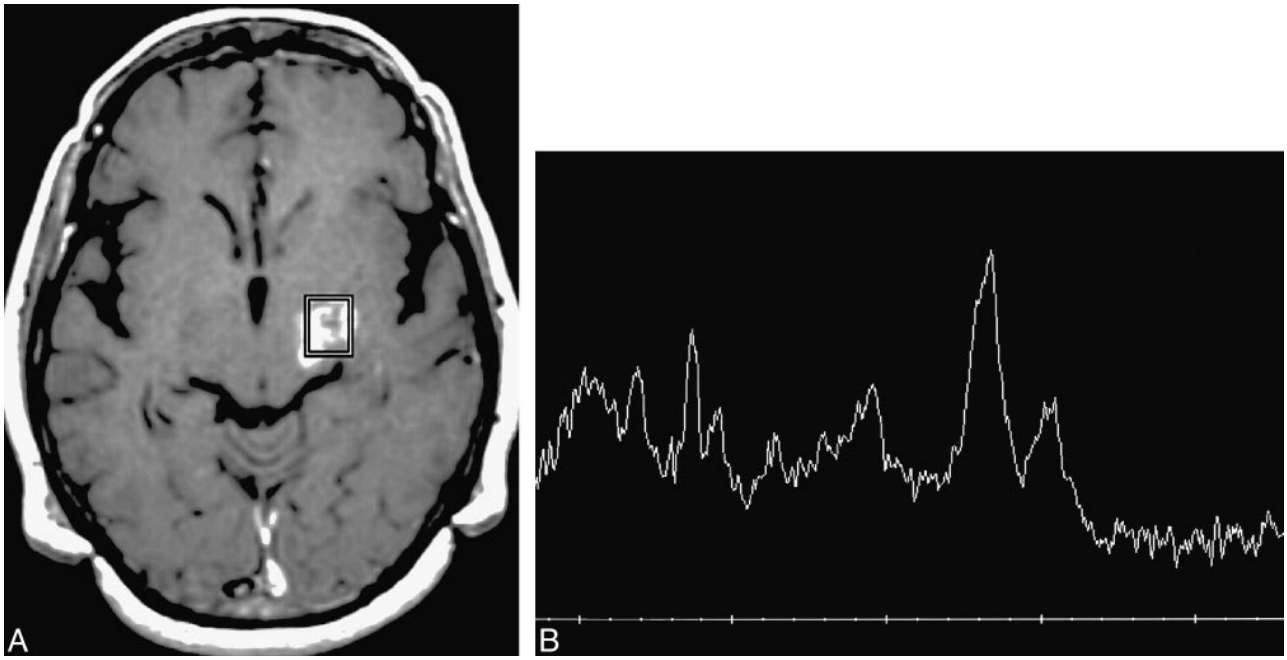

FIG 1. Patient 20: 60-year-old woman with no significant medical history.
A, Axial enhanced T1-weighted MR image reveals focal enhancement in the left cerebral peduncle and thalamus. Spectroscopy voxel is placed at the anterior margin of enhancement.
B, MR spectrum reveals elevation of the Cho/Cr ratio, elevation of the lipid/lactate peak, and marked reduction of NAA. The pattern was interpreted as consistent with tumor and was proved to be a glioblastoma multiforme at biopsy.

rized on the basis of MR spectroscopy. All were pathologically proved tumors (four primary and two recurrent glioblastomas, one primary anaplastic astrocytoma, and one metastasis). Six of the eight incorrectly categorized lesions were surgically resected; biopsies were performed in two.

The MR spectroscopy pattern in six of the 17 lesions was interpreted as consistent with tumor; all six lesions (100%) were histologically proved to be tumor (Table 1 and Fig 1). Five of those were new, untreated lesions; one was a recurrent ganglioglioma.

In 11 lesions, the MR spectroscopy pattern was interpreted as consistent with no viable tumor/necrosis (n = 10) or as indeterminate (n = 1). Three (27%) of those 11 lesions were histopathologically confirmed to be radiation necrosis with no evidence of viable tumor (Fig 2). The remaining eight lesions were all histologically confirmed tumors (five primary and two recurrent gliomas, one metastasis). In seven of those eight incorrectly categorized cases, the MR spectroscopy pattern was considered consistent with frank tissue necrosis (Figs 3 and 4). In the eighth, a histopathologically proved anaplastic astrocytoma, the NAA/Cr ratio was slightly decreased but the Cho/Cr ratio was normal. Because this spectral pattern did not meet our criteria for either the tumor or not tumor categories, it was considered indeterminate.

Data were then subdivided by the location of the spectroscopy voxel with respect to the enhancing lesion. In eight cases (five tumor, three radiation necrosis), the voxel included the edge of the enhancing lesion. Seven (88%) of those eight lesions were correctly categorized with MR spectroscopy (Table 2). This group included four glial tumors and three cases of radiation necrosis (Figs 1 and 2). The only lesion incorrectly categorized by MR spectroscopy when the voxel included the enhancing edge of the lesion was a solitary metastasis (Fig 5).

In nine lesions (all histopathologically confirmed tumors), the spectroscopy voxel was either positioned in the center of an enhancing lesion (n = 7) or included a substantial portion of a cavitary/necrotic region of the tumor (n = 2) (Figs 3 and 4). Lesion categorization was correct in only two (22%) of those nine lesions. The seven misdiagnosed lesions included five primary and two recurrent malignant gliomas.

Discussion

The ability to provide information on tissue metabolism has made single-voxel MR spectroscopy a valuable tool for evaluating brain tumors (both newly diagnosed and previously treated) and for assessing the efficacy of brain tumor therapy (1, 5–7, 12, 25). Typical MR spectroscopy changes in CNS tumors include elevated levels of choline-containing compounds (Cho, phosphorylcholine, and glycerophosphorylcholine), decreased levels of both *N*-acetyl compounds (mostly NAA) and total Cr, and variable amounts of both lipid and lactate (1–5). The key feature of tumors is elevation of the Cho peak (with a resultant increase in the Cho/Cr ratio), which most likely arises from enhanced production and destruction of cell membranes (11, 39–

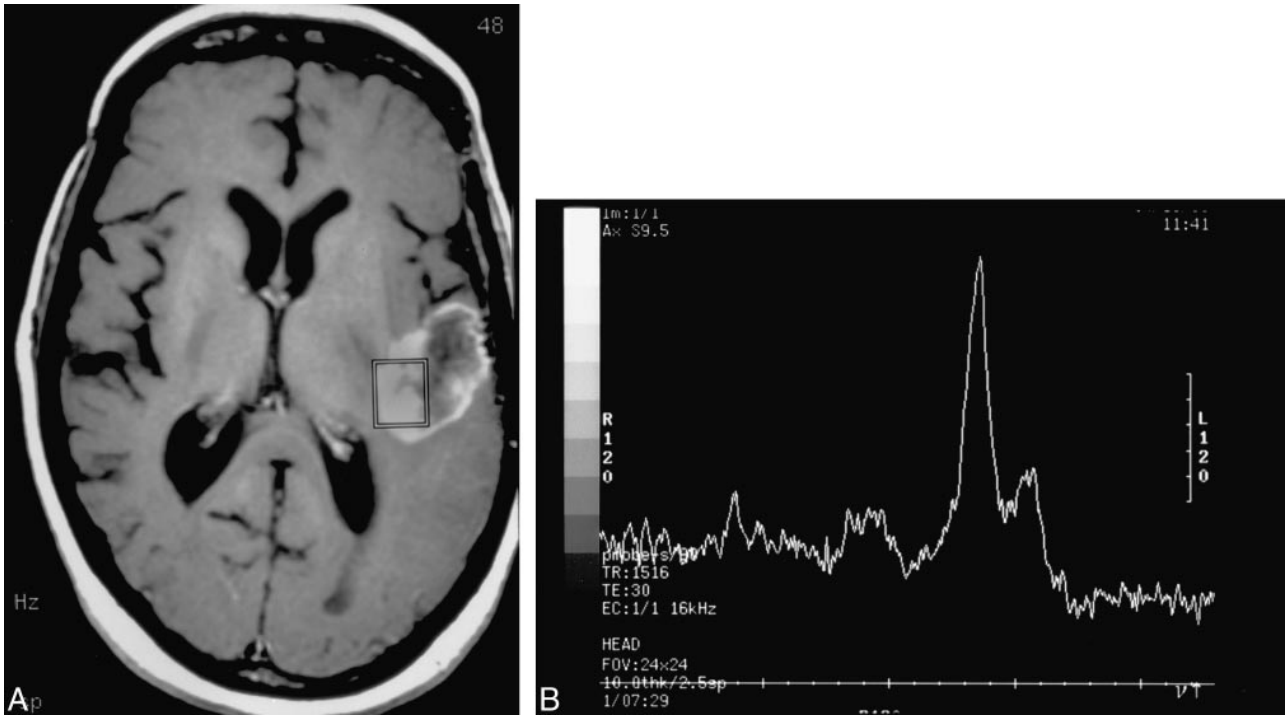

FIG 2. Patient 2: 48-year-old woman with a history of a glioblastoma multiforme treated with surgery, external beam radiation (59 Gy), and interstitial brachytherapy (58 Gy).

A, Axial T1-weighted MR image reveals enhancement of a right frontal lobe/insular lesion that has both solid and cavitary components. The spectroscopy voxel includes the medial margin of enhancement.

B, MR spectrum shows a prominent lipid/lactate peak with minimal residual Cho and Cr; NAA is absent. The pattern was thought to be consistent with radiation necrosis, and this diagnosis was confirmed at resection. This patient had subsequent follow-up spectroscopy studies at 1, 3, and 4 months that were unchanged (not shown).

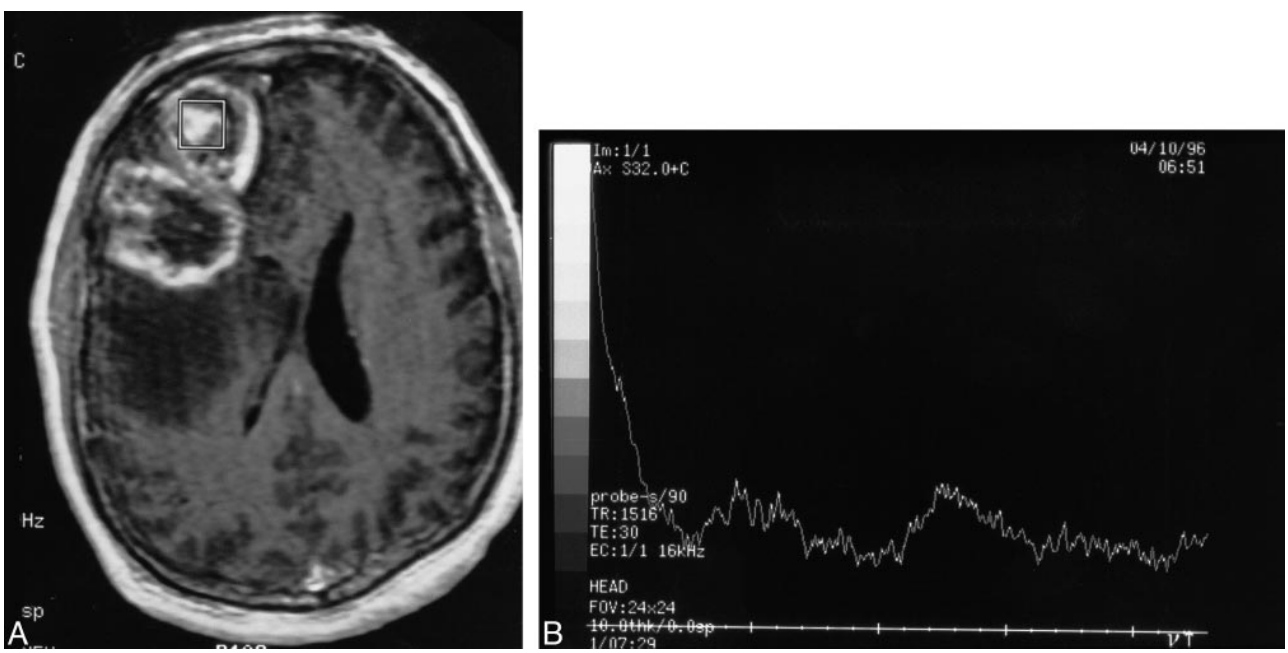

FIG 3. Patient 25: 58-year-old man with a new right frontal lobe mass.

A, Axial T1-weighted MR image reveals a multilobular cystic and solid mass in the right frontal lobe that contains peripheral and central enhancing regions. The spectroscopy voxel is positioned centrally in an enhancing portion of the tumor and does not include the enhancing edge.

B, MR spectrum reveals absence of discernible Cho, Cr, and NAA. The pattern was thought to be consistent with no tumor. The lesion was histologically shown to be a glioblastoma multiforme after resection.

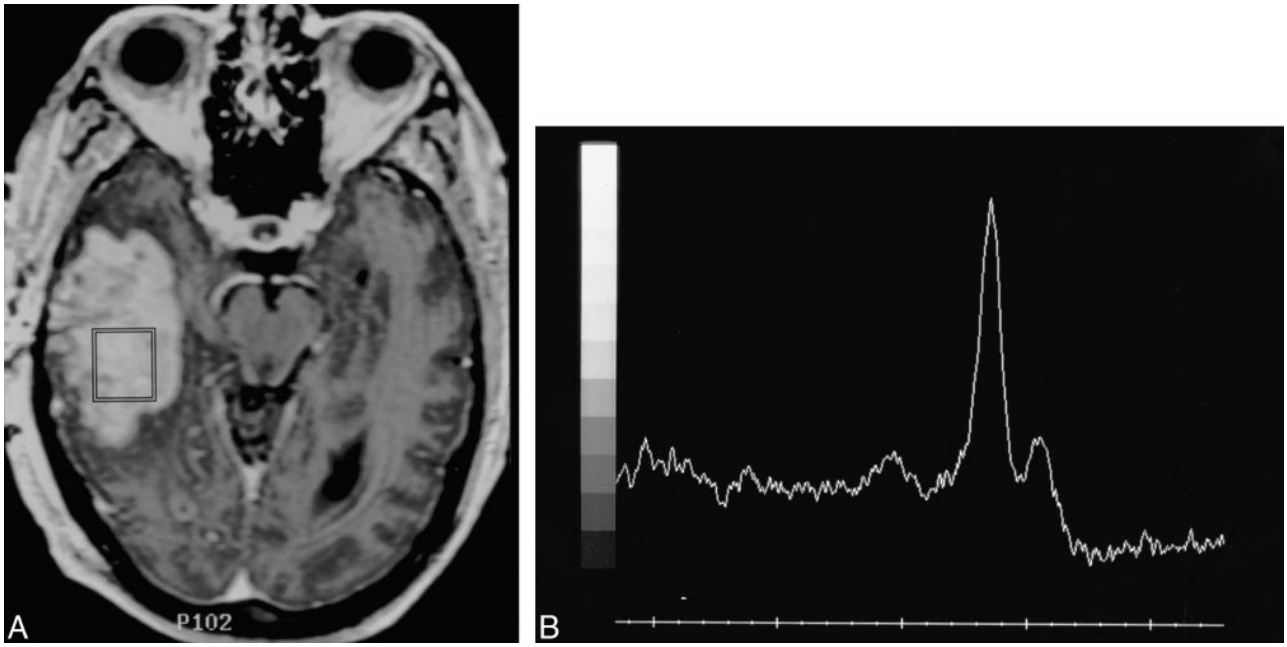

FIG 4. Patient 11: 68-year-old man with a history of a malignant glioma treated with surgical resection, external beam radiation (60 Gy), and interstitial brachytherapy (56 Gy) locally to the tumor bed.

A, Axial T1-weighted MR image obtained 8 weeks after radiation shows an enhancing mass in the right temporal lobe. There is no obvious cavitation/necrosis. The MR spectroscopy voxel is centrally positioned within the enhancing lesion.

B, The MR spectral pattern of a large lipid-lactate peak centered at 1.3 ppm and the absence of discernible Cho, Cr, or NAA were interpreted as consistent with no evidence of tumor. The lesion was completely resected and shown to be an equal mixture of glioblastoma and necrotic tissue. Because of the presence of a significant tumor component, the MR spectroscopy study was considered incorrect.

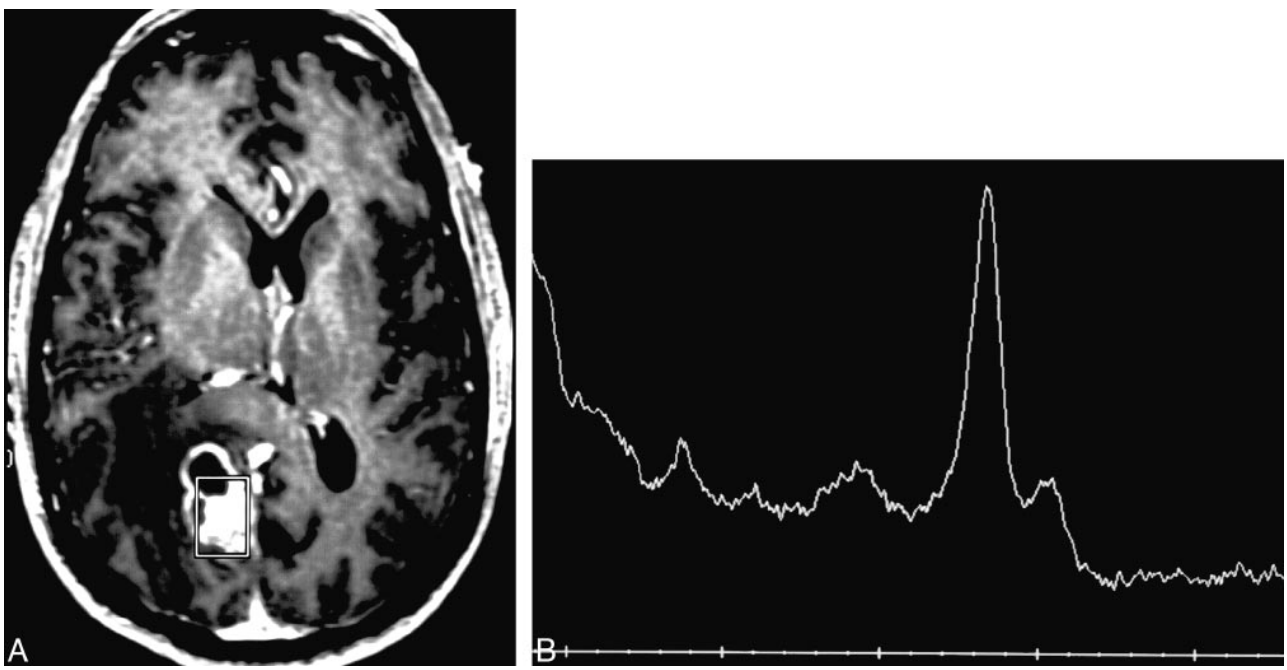

FIG 5. Patient 22: 61-year-old man with no significant medical history.

A, Axial enhanced T1-weighted MR image reveals a cystic and solid mass at the right paramedian parieto-occipital junction. The spectroscopy voxel includes the medial and posterior enhancing margins of the lesion.

B, The spectral pattern of a large lipid-lactate peak, markedly reduced Cho, and absent Cr and NAA was interpreted as consistent with no evidence of tumor. The lesion was completely resected and shown to be a solitary metastasis.

41). In contrast, radiation therapy typically results in regions of frank tissue necrosis surrounded by areas of diminished cellularity and slowed cellular proliferation (42). Spectroscopically, irradiated normal brain and tumor tissue are characterized by a decrease in the NAA level and variable changes in Cho, Cr, lipid, and lactate levels (23–26, 30–33). In cases of frank tissue or tumor necrosis, a prominent broad-based peak is often seen in the 1.2- to 1.3-ppm range. This peak, which represents a combination of lipid breakdown products and lactate, has been referred to as a ''death peak'' (29).

Unfortunately, histologic heterogeneity of both treated and untreated tumors creates the potential for sampling errors when the single-voxel technique is used. Similar biopsy sampling problems are a well-known cause for misclassification of brain tumors histologically (43–45). Our results confirm that voxel placement is a critically important factor in the reliability of MR spectra acquired with a single-voxel technique. Overall, pattern analysis of the MR spectra correctly classified only nine (53%) of 17 lesions as either tumor or not tumor. However, when the spectroscopy voxel included the margin of an enhancing lesion, pattern analysis of the spectra correctly categorized seven (88%) of eight lesions; the only misdiagnosis was a solitary metastasis. Because this was the only metastatic lesion in the study population, no meaningful assessment regarding the efficacy of single-voxel MR spectroscopy findings in the setting of metastatic disease can be made on the basis of our results.

In contrast, placement of the voxel centrally within the enhancing mass or inclusion of a substantial cavitary component within the voxel resulted in correct classification of only two (22%) of nine lesions, all of which were histologically proved tumors. Because six of those lesions were completely resected, it seems unlikely that histologic sampling error alone could account for the discrepancy. Furthermore, since six of the incorrectly classified lesions were newly diagnosed tumors, effects of prior therapy could not have been the source of error.

Also noteworthy is the fact that six patients studied had previously treated tumors. In such cases, there is a legitimate clinical need to distinguish recurrent tumor from radiation necrosis so that the appropriate therapy can be instituted in a timely fashion. The ability to distinguish recurrent tumor from radiation effects with MR spectroscopy is particularly important in light of the inability of conventional CT and MR imaging and even ^{18}F-fluorodeoxyglucose positron emission tomography to reliably make the distinction (46–53). In this study, pattern analysis of single-voxel MR spectra correctly categorized all four treated lesions (three cases of radiation necrosis, one recurrent tumor) in which the voxel included the enhancing margin of the tumor. In the remaining two patients (both with recurrent tumor), placement of the voxel in the center of the enhancing lesion resulted in incorrect categorization of the spectra by pattern analysis.

That voxel position is critical to the accuracy of MR spectroscopy findings is supported by the pathologic anatomy of tumors. High-grade glial tumors, both treated and untreated, often undergo central cavitation/necrosis, presumably because they outgrow their blood supply. Placement of the MR spectroscopy voxel in an obviously necrotic portion of a tumor, be it treated or untreated, will cause the resulting spectral pattern to be dominated by the necrotic debris. Surprisingly, we found a similar MR spectral pattern of ''necrosis'' from spectra that were acquired from apparently solid centers of some enhancing tumors. It has been suggested that mobile lipids in necrotic foci below the resolution of conventional MR imaging contribute to such lipid signal on MR spectroscopy studies (54). Still, the nearly complete absence of Cho in the spectra of such lesions is curious. Placement of a voxel at the leading edge of an enhancing lesion appears to increase the likelihood of including viable proliferating tumor in the spectroscopy volume and to decrease the chance of including microscopic foci of necrosis.

These results have potentially significant implications for the way single-voxel MR spectroscopy studies are performed in patients with known or suspected tumors. The critical dependence of voxel position on the accuracy of single-voxel MR spectroscopy findings in our study suggests that single-voxel studies in such patients should be performed after administration of contrast material so that enhancement can be used to guide voxel position. This in turn raises the important issue of the reliability of MR spectroscopy findings in the presence of gadolinium chelates. At present, this remains controversial. Using a similar STEAM sequence to ours, Taylor et al (55) concluded that gadolinium chelates do not significantly affect metabolite levels of brain tumors in vivo as measured by MR spectroscopy. More recently, Sijens et al (56) concluded that ionic gadolinium chelates selectively reduce the measured Cho level. Our own work suggests that the effect of contrast material is variable and highly dependent on the particular gadolinium chelate used (57). It should be emphasized that despite the potential effect of gadolinium on metabolite levels and ratios, MR spectroscopy still correctly identified seven of eight lesions in this study in which the voxel was correctly positioned to include the lesion margin. This suggests that MR spectroscopy can reliably separate lesions into tumor and nontumor categories despite the presence of gadolinium. Clearly, further research is needed into the nature of the effect of gadolinium on metabolite levels as measured by MR spectroscopy.

Finally, because this was a retrospective study, the results should be considered preliminary. A prospective study in which single-voxel spectra are acquired from the center and periphery of the same lesion is required to clearly define the effect of vox-

el position on the accuracy of MR spectroscopy findings.

Conclusion

Our results suggest that voxel placement in single-voxel MR spectroscopy studies of brain tumors is critical to the accurate characterization of lesion histopathology. Specifically, inclusion of the edge of an enhancing lesion in the MR spectroscopy voxel improves accuracy by maximizing the amount of viable tumor within the imaging volume. Voxel placement in the center of a lesion, whether or not frank cavitation is evident on routine MR images, increases the likelihood that cellular breakdown products will dominate the spectral pattern. As computer speed improves and fully automated spectral processing programs are developed, MR spectroscopic imaging will become more widely available and may well supplant the single-voxel technique in many institutions. Voxel position will then become less critical. Even if that occurs, our results suggest spectroscopic information obtained from the periphery of the lesion will be the most important when evaluating lesion histopathology.

Acknowledgments

This article is dedicated to the memory of Paul J. Keller, MR physicist extraodinaire, scientist, teacher, mentor, and friend.

References

1. Bruhn H, Frahm J, Gyngell ML, et al. **Noninvasive differentiation of tumors with use of localized H-1 MR spectroscopy in vivo: initial experience in patients with cerebral tumors.** *Radiology* 1989;172:541–548
2. Arnold DL, Shoubridge EA, Villemure JG, Feindel W. **Proton and phosphorus magnetic resonance spectroscopy of human astrocytomas in vivo: preliminary observations on tumor grading.** *NMR Biomed* 1990;3:184–189
3. Luyten PR, Marien AJ, Heindel W, et al. **Metabolic imaging of patients with intracranial tumors: H-1 MR spectroscopic imaging and PET.** *Radiology* 1990;176:791–799
4. Alger JR, Frank JA, Bizzi A, et al. **Metabolism of human gliomas: assessment with H-1 MR spectroscopy and F-18 fluorodeoxyglucose PET.** *Radiology* 1990;177:633–641
5. Demaerel P, Johannik K, Van Hecke P, et al. **Localized 1H NMR spectroscopy in fifty cases of newly diagnosed intracranial tumors.** *J Comput Assist Tomogr* 1991;15:67–76
6. Frahm J, Bruhn H, Hanicke W, Merboldt KD, Mursch K, Markakis E. **Localized proton NMR spectroscopy of brain tumors using short-echo time STEAM sequences.** *J Comput Assist Tomogr* 1991;15:915–922
7. Kugel H, Heindel W, Ernestus RI, Bunke J, du Mesnil R, Friedmann G. **Human brain tumors: spectral patterns detected with localized H-1 MR spectroscopy.** *Radiology* 1992;183:701–709
8. Ott D, Hennig J, Ernst T. **Human brain tumors: assessment with in vivo proton MR spectroscopy.** *Radiology* 1993;186:745–752
9. Mc Bride DQ, Miller BL, Nikas DL, et al. **Analysis of brain tumors using 1H magnetic resonance spectroscopy.** *Surg Neurol* 1995;44:137–144
10. Poptani H, Gupta RK, Roy R, Pandey R, Jain VK, Chhabra DK. **Characterization of intracranial mass lesions with in vivo proton MR spectroscopy.** *AJNR Am J Neuroradiol* 1995;16:1593–1603
11. Castillo M, Kwock L, Mukherji SK. **Clinical applications of proton MR spectroscopy.** *AJNR Am J Neuroradiol* 1996;17:1–15
12. Tien RD, Lai PH, Smith JS, Lazeyras F. **Single-voxel proton brain spectroscopy exam (PROBE/SV) in patients with primary brain tumors.** *AJR Am J Roentgenol* 1996;167:201–209
13. Preul MC, Caramanos Z, Collins DL, et al. **Accurate, noninvasive diagnosis of human brain tumors by using proton magnetic resonance spectroscopy.** *Nat Med* 1996;2:323–325
14. Shimizu H, Kumabe T, Tominaga T, et al. **Noninvasive evaluation of malignancy of brain tumors with proton MR spectroscopy.** *AJNR Am J Neuroradiol* 1996;17:737–747
15. Fulham MJ, Bizzi A, Dietz MJ, et al. **Mapping of brain tumor metabolites with proton MR spectroscopic imaging: clinical relevance.** *Radiology* 1992;185:675–686
16. Remy C, Grand S, Lai ES, et al. **1H MRS of human brain abscesses in vivo and in vitro.** *Magn Reson Med* 1995;34:508–514
17. Harada M, Tanouchi M, Miyoshi H, Nishitani H, Kannuki S. **Brain abscess observed by localized proton magnetic resonance spectroscopy.** *Magn Reson Imaging* 1994;12:1269–1274
18. Tzika AA, Ball WS Jr, Vigneron DB, Dunn RS, Kirks DR. **Clinical proton MR spectroscopy of neurodegenerative disease in childhood.** *AJNR Am J Neuroradiol* 1993;14:1261–1281
19. Moats RA, Shonk T. **Evaluation of automated MR spectroscopy: application in Alzheimer's disease.** *AJNR Am J Neuroradiol* 1995;16:1779–1782
20. Kreis R, Farrow N, Ross BD. **Localized 1H NMR spectroscopy in patients with chronic hepatic encephalopathy: analysis of changes in cerebral glutamine, choline and inositols.** *NMR Biomed* 1991;4:109–116
21. Chang L, Miller BL, Mc Bride D, et al. **Brain lesions in patients with AIDS: H-1 MR spectroscopy.** *Radiology* 1995;197:525–531
22. Chinn RJ, Wilkinson ID, Hall-Craggs MA, et al. **Toxoplasmosis and primary central nervous system lymphoma in HIV infection: diagnosis with MR spectroscopy.** *Radiology* 1995;197:649–654
23. Yousem DM, Lenkinski RE, Evans S, et al. **Proton MR spectroscopy of experimental radiation-induced white matter injury.** *J Comput Assist Tomogr* 1992;16:543–548
24. Usenius T, Usenius JP, Tenhunen M, et al. **Radiation-induced changes in human brain metabolites as studied by 1H nuclear magnetic resonance spectroscopy in vivo.** *Int J Radiat Oncol Biol Phys* 1995;33:719–724
25. Heesters MA, Kamman RL, Mooyaart EL, Go KG. **Localized proton spectroscopy of inoperable brain gliomas: response to radiation therapy.** *J Neurooncol* 1993;17:27–35
26. Szigety SK, Allen PS, Huyser-Wierenga D, Urtaasun RC. **The effect of radiation on normal human CNS as detected by NMR spectroscopy.** *Int J Radiat Oncol Biol Phys* 1993;25:695–701
27. Sijens PE, Vecht CJ, Levendag PC, Van Dijk P, Oudkerk M. **Hydrogen magnetic resonance spectroscopy follow-up after radiation therapy of human brain cancer: unexpected inverse correlation between the changes in tumor choline level and post-gadolinium magnetic resonance imaging contrast.** *Invest Radiol* 1995;30:738–744
28. Bizzi A, Movsas B, Tedeschi G, et al. **Response of non-Hodgkin lymphoma to radiation therapy: early and long term assessment with H-1 MR spectroscopic imaging.** *Radiology* 1995;194:271–276
29. Gober JR. **Noninvasive tissue characterization of brain tumors and radiation therapy using magnetic resonance spectroscopy.** *Neuroimaging Clin N Am* 1993;3:779–802
30. Taylor JS, Langston JW, Reddick WE, et al. **Clinical value of proton magnetic resonance spectroscopy for differentiating recurrent or residual brain tumor from delayed cerebral necrosis.** *Int J Radiat Oncol Biol Phys* 1996;36:1251–1261
31. Wald LL, Nelson SJ, Day MR, et al. **Serial proton magnetic resonance spectroscopy imaging of glioblastoma multiforme after brachytherapy.** *J Neurosurg* 1997;87:525–534
32. Kinoshita K, Tada E, Matsumoto K, Asari S, Ohmoto T, Itoh T. **Proton MR spectroscopy of delayed cerebral radiation in monkeys and humans after brachytherapy.** *AJNR Am J Neuroradiol* 1997;18:1753–1761
33. Esteve F, Rubin C, Grand S, Kolodie H, Le Bas JF. **Transient metabolic changes observed with proton MR spectroscopy in normal human brain after radiation therapy.** *Int J Radiat Oncol Biol Phys* 1998;40:279–286
34. Burger PC, Heinz ER, Shibata T, Kleihaus P. **Topographic anatomy and CT correlations in the untreated glioblastoma multiforme.** *J Neurosurg* 1988;68:698–704
35. Burger PC, Kleihaus P. **Cytologic composition of the untreated glioblastoma with implications for evaluation of needle biopsies.** *Cancer* 1989;63:2014–2023

36. Howells SL, Maxwell RJ, Griffiths JR. **Classification of tumour 1H NMR spectra by pattern recognition.** *NMR Biomed* 1992;5: 59–64
37. De Stefano N, Caramanos Z, Preul MC, Francis G, Antel JP, Arnold DL. **In vivo differentiation of astrocytic brain tumors and isolated demyelinating lesions of the type seen in multiple sclerosis using 1H magnetic resonance spectroscopic imaging.** *Ann Neurol* 1998;44:273–278
38. Rand SR, Prost R, Haughton V, et al. **Accuracy of single-voxel proton MR spectroscopy in distinguishing neoplastic from non-neoplastic brain lesions.** *AJNR Am J Neuroradiol* 1997;18: 1695–1704
39. Miller BL. **A review of chemical issues in 1H NMR spectroscopy: N-acetyl-L-aspartate, creatine and choline.** *NMR Biomed* 1991;4:47–52
40. Miller BL, Chang L, Booth R, et al. **In vivo 1H MRS choline: correlation with in vitro chemistry/histology.** *Life Sci* 1996;58: 1929–1935
41. Chang L, Mc Bride D, Miller BL, et al. **Localized in vivo 1H magnetic resonance spectroscopy and in vitro analyses of heterogeneous brain tumors.** *J Neuroimaging* 1995;5:157–163
42. Burger PC, Scheithauer BW. **Tumors of the central nervous system.** In: Rosai J, ed. *Atlas of Tumor Pathology*. Third series, fascicle 10. Washington, DC: Armed Forces Institute of Pathology; 1994:25–77
43. Burger PC, Kleihues P. **Cytologic composition of the untreated glioblastoma with implications for evaluation of needle biopsies.** *Cancer* 1989;63:2014–2023
44. Paulus W, Peiffer J. **Intratumoral histologic heterogeneity of gliomas: a quantitative study.** *Cancer* 1989;64:442–447
45. Glantz MJ, Burger PC, Herndon JE II, et al. **Influence of the type of surgery on the histologic diagnosis in patients with anaplastic gliomas.** *Neurology* 1991;41:1741–1744
46. Dooms GC, Hecht S, Brant-Zawadzki M, Berthiaume Y, Norman D, Newton TH. **Brain radiation lesions: MR imaging.** *Radiology* 1986;158:149–155
47. Mikhael MA. **Radiation necrosis of the brain: correlation between, computed tomography, pathology and dose distribution.** *J Comput Assist Tomogr* 1978;2:71–80
48. Kingsley DPE, Kendall BE. **CT of the adverse effects of therapeutic radiation of the central nervous system.** *AJNR Am J Neuroradiol* 1981;2:453–460
49. van Dellen JR, Danziger A. **Failure of computerized tomography to differentiate between radiation necrosis and cerebral tumour.** *S Afr Med J* 1978;53:171–172
50. Valk PE, Dillon WP. **Radiation injury of the brain.** *AJNR Am J Neuroradiol* 1991;12:45–62
51. Ricci PE, Karis JP, Heiserman, Fram EK, Bice AN, Drayer BP. **Differentiating recurrent tumor from radiation necrosis: time for re-evaluation of positron emission tomography?** *AJNR Am J Neuroradiol* 1998;19:407–413
52. Kahn D, Follett KA, Bushnell DL, et al. **Diagnosis of recurrent brain tumor: value of ^{201}Tl SPECT vs ^{18}F-fluorodeoxyglucose PET.** *AJR Am J Roentgenol* 1994;163:1459–1465
53. Olivero WC, Dulebohn SC, Lister JR. **The use of PET in evaluating patients with primary brain tumours: is it useful?** *J Neurol Neurosurg Psychiatry* 1995;58:250–252
54. Kuesel AC, Sutherland GR, Halliday W, Smith ICP. **1H MRS of high grade astrocytoma: mobile lipid accumulation in necrotic tissue.** *NMR Biomed* 1994;7:149–155
55. Taylor JS, Reddick WE, Kingsley PB, Ogg RJ. **Proton MRS after gadolinium contrast agent.** Third Scientific Meeting and Exhibition of the Society of Magnetic Resonance, In: *Proceedings of the Society of Magnetic Resonance: Nice, France, August 19–25, 1995.*
56. Sijens PE, van den Bent MJ, Nowak PJCM, van Dijk P, Oudkerk M. **1H chemical shift imaging reveals loss of brain tumor choline signal after administration of Gd-contrast.** *Magn Reson Med* 1997;37:222–225
57. Ricci PE, Schepkin VD, Elster AD, Hamilton CA. **Effect of three gadolinium chelates on cerebral metabolite levels measured by single-voxel proton MR spectroscopy.** In: *Book of Abstracts, 37th Annual Meeting of the American Society of Neuroradiology, San Diego, CA, May 22–28, 1999.* Oak Brook, IL: American Society of Neuroradiology; 1999